Experiment and Simulation of Impregnated No-Insulation REBCO Pancake Coil

So Noguchi, Katsutoshi Monma, Sadanori Iwai, Hiroshi Miyazaki, Taizo Tosaka, Shunji Nomura, Tsutomu Kurusu, Hiroshi Ueda, Atsushi Ishiyama, Shinichi Urayama, and Hidenao Fukuyama

***Abstract*—It is important to investigate the stability and behavior of an epoxy-resin-impregnated no-insulation (NI) REBCO pancake coil in order to implement high-field applications, such as ultra-high-field magnetic resonance imaging. We have performed sudden discharging and overcurrent tests for the impregnated NI REBCO pancake coil. From the discharging test, the contact resistivity is estimated, and it changes depending on the initial current. From the overcurrent test, the high thermal stability of the impregnated NI REBCO pancake coil is confirmed. The REBCO pancake coil is charged up to 67 A though the critical current is only 46 A, and no degradation has been found.**

To investigate in detail the electromagnetic behavior of an impregnated NI REBCO pancake coil, the simulation is performed by means of the partial element equivalent circuit (PEEC) model. In the sudden discharging test, the simulation results for the case of lower initial current are in good agreement with the experimental data. As can be inferred from the simulation results, the current drastically decreases from the inside of the impregnated NI REBCO pancake coil. The result of the overcurrent simulation is almost identical to the experimental one. However, since the contact resistivity is presumed to be constant in the simulation, the difference is observed in the high current region.

***Index Terms*—Epoxy resin impregnation, high-temperature superconducting coil, no-insulation technique.**

I. Introduction

THE NO-INSULATION (NI) WINDING TECHNIQUE is a promising quench-protection method for REBCO pancake coils. The NI technique was proposed for LTS coils [1], and later it attracted attention for NI REBCO pancake coils. Since Hahn et al. published the experimental results of the overcurrent test of the pancake coil without insulation between turns [2], many experimental results concerning NI REBCO pancake coils have been reported [3], [4]. These experiments have shown a high thermal stability, and so the NI winding technique was applied to some REBCO magnets, e.g., a 8.7-T/91-mm NMR magnet, 9-T/78-mm NMR magnet, 26-T/35-mm NMR magnet, etc. [5]. It will be also used in many applications of the REBCO pancake coils.

With the development of the NI winding technique, it is necessary to clarify the electromagnetic and thermal behaviors of NI REBCO pancake coils. A few simulation methods for NI REBCO pancake coils have been developed for clarification of the high stability mechanism [2], [6]. The simple equivalent circuit model is a facile analysis method [2]; however, the current behavior inside the NI REBCO pancake coil is not considered. We have developed the partial element equivalent circuit (PEEC) model to investigate in detail the behavior of NI REBCO pancake coils for the discharging/charging test and the overcurrent test as well [6], [7]. The simulation results also revealed the mechanism of the high stability.

To apply the NI winding technique to large-size REBCO pancake coils for commercial applications with conduction-cooling system, such as an ultra-high-field HTS MRI [8], it is required to impregnate the NI REBCO pancake coils with epoxy resin. Therefore, we have done sudden discharging and overcurrent tests on an impregnated NI REBCO pancake coil. The NI winding technique gives a high stability even to NI REBCO pancake coils impregnated with epoxy resin, i.e. it is possible to flow a 1.45 times larger current, without burning-out, than the coil critical current. The experiment reveals the NI winding technique is effective even in the impregnated NI REBCO pancakes. The experimental results are compared with the simulation results of the PEEC model, and we confirm the validity of the PEEC model even for the impregnated NI REBCO pancake coils.

II. Experimental Setup and Simulation Condition

A. Experimental Setup

The specifications of our impregnated NI REBCO pancake coil are given in Table I. The coil itself is shown in Fig. 1, and the circuit in the experiments is shown in Fig. 2. The REBCO pancake coil was impregnated with epoxy resin. The epoxy impregnation was applied during the winding process. The measured coil *V-I* characteristic is given in Fig. 3. The impregnated NI REBCO pancake coil is cooled in a liquid nitrogen bath. The current from the power supply to the NI REBCO pancake coil cuts off using the direct current circuit breakers (DCCB) in the sudden discharging test. Because the current is measured using a shunt resistor, the current flowing

Automatically generated dates of receipt and acceptance will be placed here; authors do not produce these dates. This work was supported by the Ministry of Economy, Trade and Industry of the Japanese Government and Agency for Medical Research and Development. Corresponding author: So Noguchi.

S. Noguchi and K. Monma are with Graduate School of Information Science and Technology, Hokkaido University, Sapporo 060-0814, Japan (e-mail: noguchi@ssi.ist.hokudai.ac.jp).

S. Iwai, H. Miyazaki, T. Tosaka, S. Nomura, and T. Kurusu are with Toshiba Corporation, Yokohama 230-0045, Japan.

H. Ueda is with Osaka University, Osaka 565-0047, Japan.

A. Ishiyama is with Waseda University, Tokyo 169-8555, Japan.

S. Urayama and H. Fukuyama are with Kyoto University, Kyoto 606-8507, Japan.

TABLE I
SPECIFICATIONS OF IMPREGNATED NI PANCAKE COIL

Tape width (mm)	4
Tape thickness (mm)	0.1
Tape length (m)	8.3
Tape I_c (77 K, s.f.) (A)	110
Inner diameter (mm)	50
Outer diameter (mm)	60
Number of turns	48
Inductance (μH)	210
Coil I_c (77 K, s.f.) (A)	46
Coil *n*-value	22

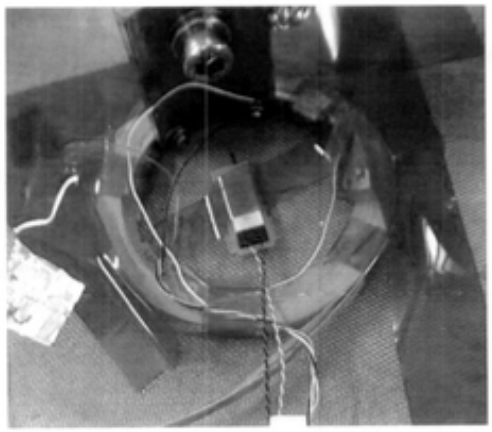

Fig. 1. The photo of the NI REBCO pancake coil impregnated with epoxy resin.

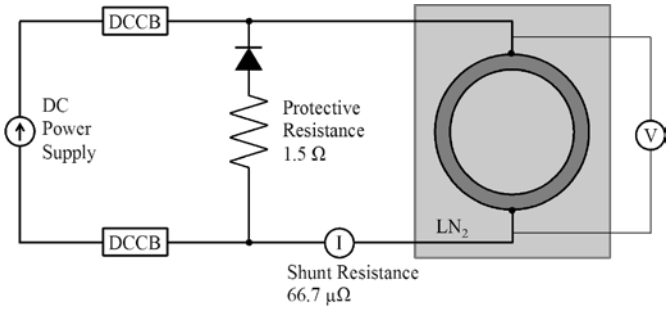

Fig. 2. Experimental circuit for sudden discharging test of impregnated NI REBCO pancake coil.

inside the coil is unknown during the sudden discharging test.

B. Simulation Condition

The PEEC model, as shown in Fig. 4, is employed as the simulation method. The number of azimuthal divisions is 24, the simulation time step is 0.01 s, and the *V-I* characteristic fitting curve as shown in Fig. 3 is used.

III. SUDDEN DISCHARGING TEST

A. Experimental Results

In the sudden discharging test, the voltage of the coil, the on-axis field, and the current of the shunt resistance is measured at the initial current value of 20 A, 30 A, 40 A, and 50A. The on-axis field is measured with a Hall sensor. Figs. 5 and 6 show the waveform of the coil voltage and the on-axis field at initial currents of 20 and 50 A, respectively.

Fig. 7 shows the normalized on-axis magnetic field at the initial current of 20 A, 30 A, 40 A, and 50 A. Table II lists the

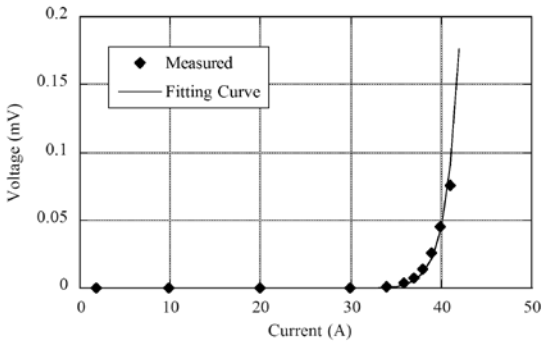

Fig. 3. Measured coil *V–I* characteristic and its fitting curve. The Coil I_c is 46 A, and *n*-value 22.

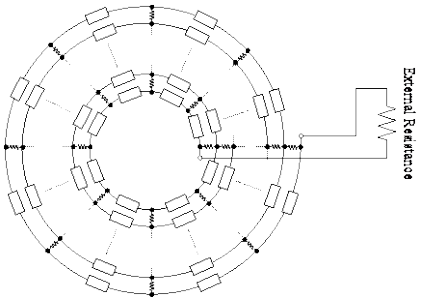

Fig. 4. The PEEC model with an external resistance of 1.5 Ω.

time constant, the contact resistance, and the contact resistivity, obtained from Fig. 6. The contact resistance is obtained from the time constant [2], and the effective contact resistivity is derived according to [9]. The obtained values are greater than the value of 70 μΩ•cm^2 in [9]. In the experiment, the contact resistivity changes depending on the initial current. It causes the generation of the flux-flow resistance or a little increase of the temperature with the increase of the initial current.

B. Simulation Results

Figs. 5 and 6 show the on-axis field and voltage as a function of time at the initial current of 20 A and 50 A, respectively. The contact resistivity is taken equal to 106 μΩ•cm^2 at 20 A and 144 μΩ•cm^2 at 50 A, respectively. The simulation result of 20-A initial current is identical to the experimental one; however, the 50-A simulation result is a little different from the experimental one. In the PEEC simulation, the *V-I* characteristic of the impregnated NI pancake coil is taken into account, so it is concluded that the change of the contact resistivity on the initial current is not caused by the flux-flow resistance. A reason for the contact resistivity increase does not become clear through the PEEC simulation. We have to keep looking for it.

The azimuthal and radial current distribution of the 20-A initial current are represented in Figs. 8 and 9, respectively. Both the azimuthal and radial current rapidly attenuates from the inside of the coil.

Fig. 10 shows the normalized on-axis magnetic field at the initial current value of 20 A, 30 A, 40 A, and 50 A. The time constants which are obtained from Fig. 8 are shown in Table II, and these values agree with the experimental ones well.

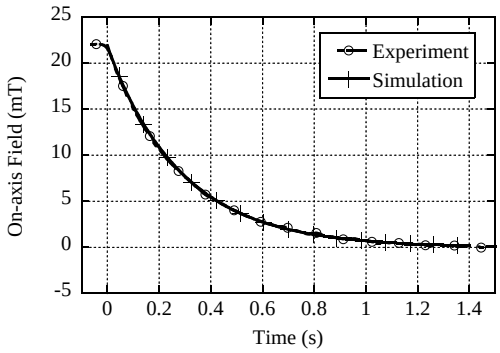

(a) Experimental and simulated on-axis magnetic field

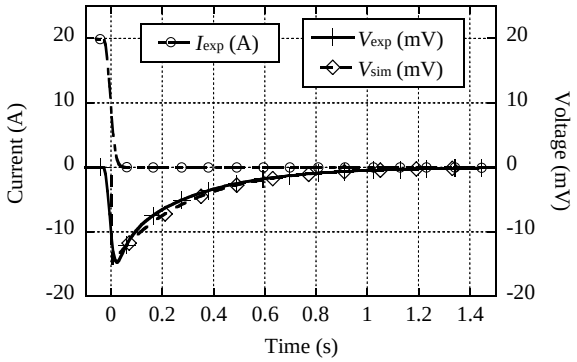

(b) Coil voltage and current

Fig. 5. The sudden discharging test at the initial current of 20 A. (a) The experimental and simulated on-axis fields. The two plots are almost identical. (b) The measured current I_{exp} at the shunt resistance, the experimental coil voltage V_{exp}, and the simulated voltage V_{sim}.

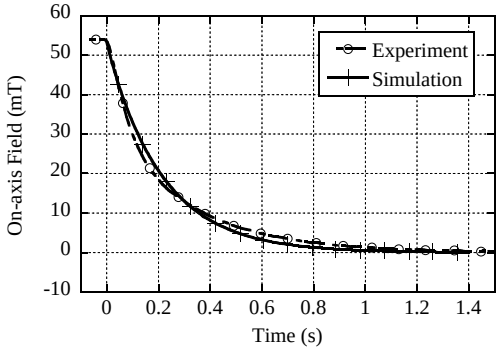

(a) Experimental and simulated on-axis magnetic field

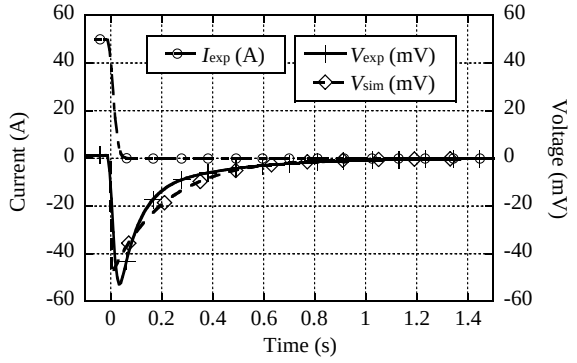

(b) Coil voltage and current

Fig. 6. The sudden discharging test at an initial current of 50 A. (a) The experimental and the simulated on-axis field. (b) The measured current I_{exp} at the shunt resistance, the experimental coil voltage V_{exp}, and the simulated voltage V_{sim}.

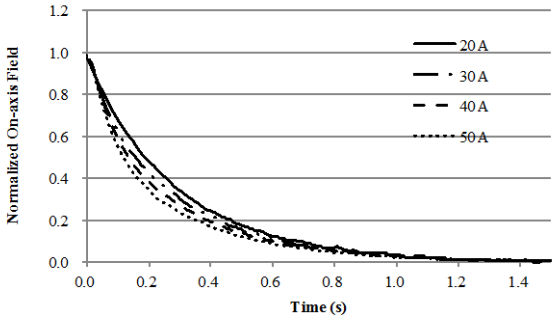

Fig. 7. The normalized on-axis magnetic field of sudden discharging experiment.

TABLE II
TIME CONSTANT, CONTACT RESISTANCE, AND RESISTIVITY

Initial current (A)	20	30	40	50
Time constant (s) [exp.]	0.285	0.255	0.230	0.210
Time constant (s) [sim.]	0.29	0.26	0.23	0.21
Contact resistance (μΩ)	736.8	823.5	913.0	1000.0
Contact resistivity (μΩ•cm^2)	106	118	131	144

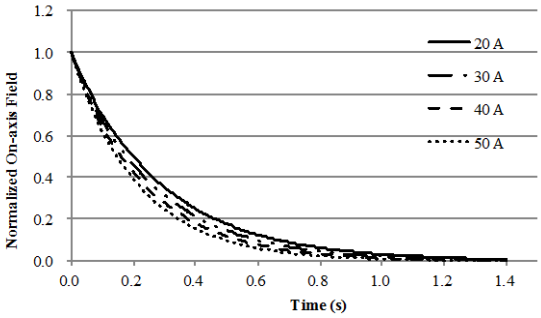

Fig. 10. The normalized on-axis magnetic field of sudden discharging simulation.

IV. OVERCURRENT TEST

A. Experimental Results

The overcurrent test is done for the epoxy-resin-impregnated NI pancake coil. The current gradually increases from 0 to 67 A, although the coil critical current I_c is 46 A. Fig. 11 shows the waveform of the current and on-axis field on the overcurrent test. Fig. 12 shows the relation between the current and on-axis field. The on-axis field linearly increases below the coil I_c of 46 A; however, the saturation of the on-axis field is observed beyond the coil I_c. At 60 A, the on-axis field drastically drops down, but it may include a measurement error. Over 60 A, the on-axis field gradually decreases because the flux-flow resistivity increases.

The impregnated NI REBCO pancake coil suffers no damage through the overcurrent test. The high thermal stability of the epoxy-resin-impregnated NI REBCO pancake coil is revealed.

B. Simulation Results

Fig. 12 shows the simulated on-axis magnetic field as a function of current, obtained by the PEEC model. The on-axis magnetic field gradually begins saturating at approximately 46 A, like the experimental result. The simulated central magnetic field from 46 to 60 A is lower than the experimental

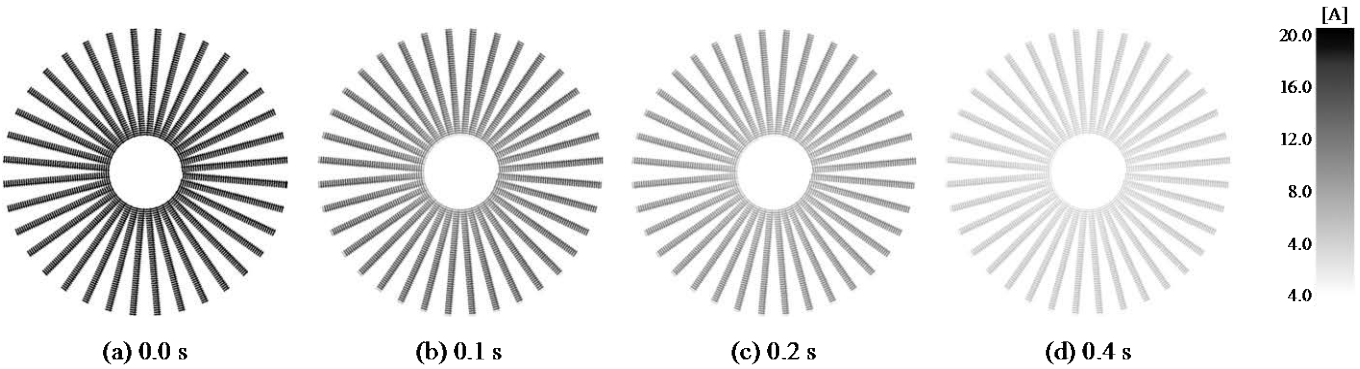

Fig. 8. Azimuthal current distribution at 20-A initial current (not to scale).

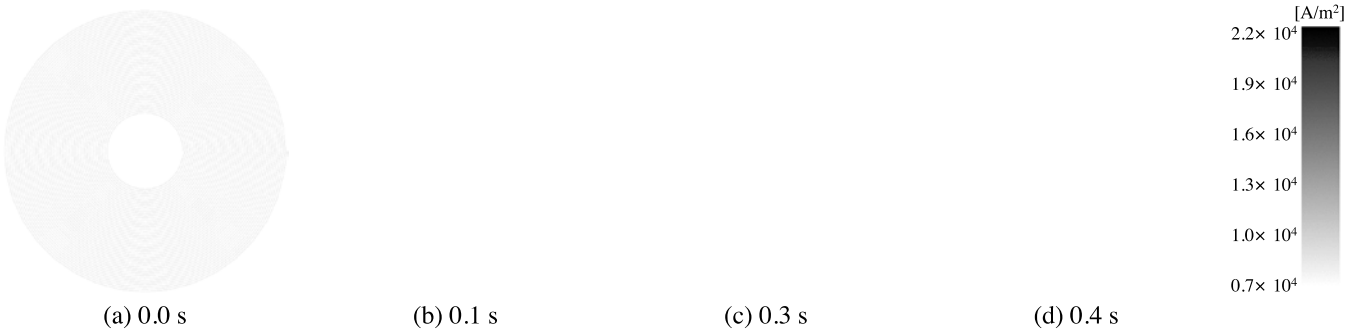

Fig. 9. Radial current density distribution at 20-A initial current (not to scale).

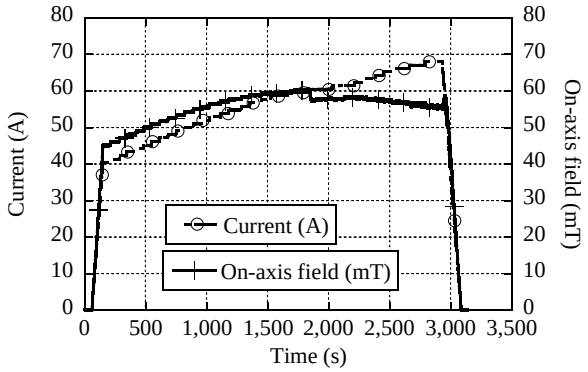

Fig. 11. The current and on-axis field in the overcurrent test.

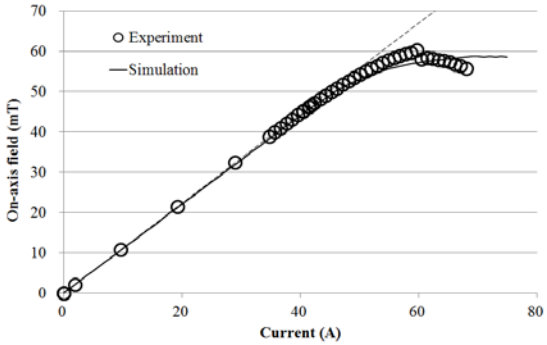

Fig. 12. The on-axis magnetic field as a function of current.

one. Since the contact resistivity value of 106 μΩ•cm^2 is held constant in the overcurrent simulation, the azimuthal current largely decreases with the increase of the current, as compared with the measurement. The increase of the contact resistivity has to be taken into account for the accurate simulation.

V. Conclusion

To understand the high stability of the impregnated no-insulation (NI) REBCO pancake coil, the sudden discharging and overcurrent tests are performed. Through the overcurrent testing, the NI winding technique works to enhance the thermal stability. Although the coil critical current is 46 A, the transport current can be increased up to 67 A without damage.

From the sudden discharging test, the effective contact resistivity is estimated at a number of the initial current values. The higher the initial current is, the larger the estimated contact resistivity is. We need to investigate the increase of the estimated contact resistivity more.

We simulate the electromagnetic behavior of the impregnated NI REBCO pancake coil using the partial element equivalent circuit (PEEC) model. The PEEC simulation results of the sudden discharging test agree with the experimental results well. The current distribution is shown during sudden coil discharge. The simulation result of the overcurrent test is also shown. From the simulation results of both the tests, the simulation condition in the range over the coil critical current has to be reconsidered, e.g. the thermal simulation is coupled with the PEEC model.

References

[1] A. V. Dudarev, A. V. Garvrilin, V. I. Keilin, et al., "Superconducting windings with 'short-circuited' turns," *Inst. Phys. Conf,.* Ser. 158, pp. 1615-1618, 1997.

[2] S. Hahn, D. K. Park, J. Bascuñán, and Y. Iwasa, "HTS pancake coils without turn-to-turn insulation," *IEEE Trans. Appl. Supercond*., vol. 21, no. 3, pp. 1592–1595, Jun. 2011.

[3] J. Song, S. Hahn, Y. Kim, D. Miyagi, J. Voccio, J. Bascuñán, H. Lee, and Y. Iwasa, “Dynamic response of no-insulation and partial-insulation coils for HTS wind power generator,” *IEEE Trans. Appl. Supercond.*, vol. 25, no. 3, Jun. 2015, Art. ID. 5202905.

[4] Y. Kim, S. Hahn, K. L. Kim, O. J. Kwon, and H. Lee, “Investigation of HTS Racetrack Coil Without Turn-to-Turn Insulation for Superconducting Rotating Machines,” *IEEE Trans. Appl. Supercond.*, vol. 22, no. 3, Jun. 2012, Art. ID. 5200604.

[5] S. Hahn and Y. Iwasa, “No-Insulation HTS Winding Technique for High-Field NMR Magnets,” presented at EUCAS 2015 (1A.OS.L2.2), Lyon, Sep. 2015.

[6] X. Wang, T. Wang, E. Nakada, A. Ishiyama, R. Itoh, and S. Noguchi, “Charging behavior in no-insulation REBCO pancake coils,” *IEEE Trans. Appl. Supercond.*, vol. 25, no. 3, Jun. 2015, Art. ID. 4601805.

[7] T. Wang, S. Noguchi, X. Wang, I. Arakawa, K. Minami, K. Monma, A. Ishiyama, S. Hahn, and Y. Iwasa, “Analyses of transient behaviors of no-insulation REBCO pancake coils during sudden discharging and overcurrent,” *IEEE Trans. Appl. Supercond.*, vol. 25, no. 3, Jun. 2015, Art. ID. 4603409.

[8] T. Tosaka, H. Miyazaki, S. Iwai, Y. Otani, M. Takahashi, K. Tasaki, S. Nomura, T. Kurusu, H. Ueda, S. Noguchi, A. Ishiyama, S. Urayama, and H. Fukuyama, “Project overview of HTS magnet for Ultra-high field MRI system,” *Physics Procedia*, vol. 65, pp. 217–220, Nov. 2014.

[9] X. Wang, S. Hahn, Y. Kim, J. Bascuñán, J. Voccio, H. Lee, and Y. Iwasa, “Turn-to-turn contact characteristics for an equivalent circuit model of no-insulation ReBCO pancake coil,” *Supercond. Sci. Technol.*, vol. 26, no. 3, Mar. 2013, Art. ID. 035012.